

Synthesis and Characterization of Cd–DMSO Complex Capped CdS Nanoparticles

Manoj E. Wankhede and Santosh K. Haram*

Department of Chemistry, University of Mumbai, Vidyanagar, Mumbai 400098, India

Received July 15, 2002. Revised Manuscript Received December 18, 2002

We report here the capping of cadmium sulfide nanoparticles (Q-CdS) with a Cd–DMSO complex as a consequence of particle preparation in dimethyl sulfoxide (DMSO). A characteristic sharp peak at 367 nm in the UV–vis for Q-CdS showed a gradual blue shift of ca. 41 nm, indicating the decrease in the particle size with time instead of the expected red shift for flocculation. Erosion of the particles was attributed to the reaction of CdS with DMSO to form a Cd–DMSO complex. FTIR spectra recorded for flocculated Q-CdS gave major peaks at 617, 800, 1109, 1261, 1408, and 1561 cm^{-1} which were attributed to the presence of Cd–DMSO complex and acetate ions on the particle surface. The anti-stoke shift of S=O stretching frequency for particle-associated DMSO indicated that the bonding is through a sulfur moiety. On the basis of results from thermal and postannealed IR spectral analyses, the formation of a stable Cd–DMSO complex on the particle surface was inferred. The observed solution stability was attributed to the particle surface passivation by the complex. The kinetic studies of the reaction between Q-CdS and DMSO revealed that the reaction is second order with a rate constant of ca. $2 \times 10^{-6} \text{ L mol}^{-1} \text{ s}^{-1}$.

Introduction

During the past two decades, semiconductor nanoparticles or quantum dots, in particular those of the cadmium chalcogenides, have attracted considerable attention due to their tunable electronic properties as a function of size, the so-called quantum size effect.^{1,2} There is an exhaustive supply of literature available for particle preparation in various media and with a variety of capping agents.^{3–10} A crux in the development of a particle preparation method is effective control over particle size and dispersity without compromising optoelectronic properties. Among these, the synthetic method developed by Bawendi et al.⁹ and recently refined by Peng et al.¹⁰ involving particle stabilization by tri-*n*-octylphosphine oxide (TOPO) has been extremely successful. It enables precise particle size and monodispersity control,⁹ and does not degrade the optoelectronic properties.¹¹ Such TOPO-coated Q-CdSe particles have been used for stimulated light emission.¹²

The excellent stability and monodispersity of these particles have been attributed to surface passivation by alkyl phosphine oxide. It is interesting to consider whether sulfoxides such as DMSO, a homologue of alkyl phosphine oxide, could have a similar stabilizing effect on Q particles. To date, there are few reports that detail an interaction of DMSO with the Q-CdS surface when the sols are prepared in DMSO. Using 2D NMR spectroscopy, Kotov et al.¹³ demonstrated that the particle surface is occupied by ethyl hexanoate from the cadmium 2-ethyl hexanoate precursor used in synthesis. DMSO was also found to be adsorbed on the surface. Hode et al.¹⁴ suggested the formation of a bridging complex of acetate with surface Cd²⁺ of Q-CdS in addition to the adsorption of DMSO through oxygen linkage. Here, we report that Q-CdS itself reacts with DMSO when the sols are prepared in this solvent, leading to a decrease in Q-CdS size due to the formation of a shell of Cd–DMSO complex on Q-CdS core. Thus, in this case, the interaction is not just a topographical one.

2.0 Experimental Section

- (1) Brus, L. E. *J. Chem. Phys.* **1983**, *79*, 5566.
- (2) Brus, L. E. *J. Chem. Phys.* **1984**, *80*, 4403.
- (3) Vossmeye, T.; Katsikas, L.; Giersig, M.; Popovic, I. G.; Diesner, K.; Chemeddine, A.; Eychmuller, A.; Weller, H. *J. Phys. Chem.* **1994**, *98*, 7665.
- (4) Minti, H.; Eyal, M.; Reisfeld, R. *Chem. Phys. Lett.* **1991**, *183*, 277.
- (5) Huang, J.; Yang, Y.; Yang, B.; Liu, S.; Shen, J. *Polym. Bull.* **1996**, *37*, 679.
- (6) Kakuta, N.; White, J. M.; Campion, A.; Fox, M. A.; Webber, S. E. *J. Phys. Chem.* **1985**, *89*, 48.
- (7) Lianos, P.; Thomas, J. K. *J. Colloid Interface Sci.* **1987**, *117*, 505.
- (8) Herron, N.; Wang, Y.; Eddy, M. M.; Stucky, G. D.; Cox, D. E.; Moller, K.; Bein, T. *J. Am. Chem. Soc.* **1989**, *111*, 350.
- (9) Murray, C. B.; Norris, D. J.; Bawendi, M. G. *J. Am. Chem. Soc.* **1993**, *115*, 8706.
- (10) Peng, Z. A.; Peng, X. *J. Am. Chem. Soc.* **2001**, *123*, 183.

2.1 Materials. Cadmium acetate dihydrate (Merck), sodium sulfide flakes (S. D. Fine Chemicals, India), dimethyl sulfoxide (S. D. Fine), and all the other chemicals were of analytical reagent grade and used as received without any further

- (11) Murray, C. B.; Kagan, C. R.; Bawendi, M. G. *Annu. Rev. Mater. Sci.* **2000**, *30*, 545.
- (12) Klimov, V. I.; Mikhailovsky, A. A.; Xu, S.; Malko, A.; Hollingsworth, J. A.; Leatherdale, C. A.; Eisler, H. J.; Bawendi, M. G. *Science* **2000**, *314*.
- (13) Diaz, D.; Rivera, M.; Ni, T.; Rodriguez, J.-C.; Castillo-Blum, S.-E.; Nagesha, D.; Robles, J.; Alvarez-Fregoso, O.-J.; Kotov, N. A. *J. Phys. Chem. B* **1999**, *103*, 9854.
- (14) Elbaum, R.; Vega, S.; Hodes, G. *Chem. Mater.* **2001**, *13*, 2272.

purification. The solutions of cadmium acetate dihydrate ($\text{Cd}(\text{OAc})_2$) and sodium sulfide (Na_2S) were prepared by dissolving an appropriate quantity of the compounds in DMSO. Cadmium acetate dihydrate dissolves spontaneously, whereas the dissolution of sodium sulfide requires sonication for several minutes at room temperature. A stock solution of cadmium acetate in DMSO could be stored and used as needed. However, the solution of Na_2S was prepared freshly and used immediately. Some reactions were carried out under N_2 atmosphere. N_2 used was of high purity (Indian Oxygen Ltd, IOLAR grade, O_2 less than 5 ppm). To remove the last traces of O_2 and moisture, it was passed through Fischer's solution and fused CaCl_2 scrubbers, respectively, prior to use.

2.2 Preparation of CdS Sols in DMSO. CdS sols were prepared by mixing $\text{Cd}(\text{OAc})_2$ and fresh Na_2S solutions in DMSO at room temperature. Typically, 10 mL of $\text{Cd}(\text{OAc})_2$ (10 mM) was transferred into a 250-mL Erlenmeyer flask and 10 mL of Na_2S (10 mM) was added dropwise with a constant stirring. Within minutes, the solution developed to a transparent pale yellow, which was nonopalescent under ambient room light but exhibited pronounced Tyndall effect when directly exposed to a beam of He–Ne laser. To ensure completion of the reaction, the sols were allowed to ripen for 5 h prior to characterization. For UV–vis analyses, the sol was diluted 10 times (effective concentration of Cd^{2+} and S^{2-} in the final bath was 0.5 mM) to limit the absorbance value within the linear range. For steady-state photoluminescence (PL) measurements, the sol was diluted 50 times (effective concentration of Cd^{2+} and S^{2-} was 0.1 mM), to minimize the self-quenching rate, which dominates at higher concentrations and contributes to line broadening. To study the effect of O_2 on the reaction, some preparations were carried out in N_2 and O_2 atmospheres. The setup used is described in the Supporting Information.

To obtain a powder sample for material characterization, the prepared Q-CdS sol was flocculated using anti-solvents, viz. acetone or 2-propanol.^{3,9} A 20-mL aliquot of sol (5 mM) was titrated against acetone with constant stirring. Typically, 40 mL of acetone was required for the first appearance of turbidity, which was allowed to settle overnight. This was then centrifuged at 8000 rpm for 15 min and decanted. The resultant precipitate was washed several times with a copious amount of acetone, dried, and stored under vacuum for further analysis.

2.3 Characterization. Powder X-ray diffractograms (XRD) on the dried precipitate were recorded using a JEOL JDX-8030 X-ray diffractometer having $\text{Cu K}\alpha$ source (40 kV and 20 mA). Samples were prepared by sprinkling the precipitate over pre-greased glass slides. The diffractograms were recorded between angles 20° and 70° with a scan rate of 2 s per step (0.05° step).

For routine characterization and reaction kinetics studies, UV–vis (Shimadzu UV-2401PC) spectra were recorded for the sols at the stipulated time intervals. Steady state photoluminescence (PL) spectra were recorded at room temperature using a Shimadzu RF-5301PC spectrophotometer. Excitation wavelengths were typically 300 and 340 nm, respectively, and emission spectra were recorded between 300 and 900 nm. For the sols prepared under controlled atmosphere (N_2 and O_2), samples were sealed in Teflon-corked cuvettes and measurements were performed periodically.

For IR spectroscopic measurements, ca. 10 mg of the dried precipitate was mixed with ca. 100 mg of spectroscopic-grade potassium bromide, and the resultant suspension was ground into a fine powder by using a mortar and pestle. A portion of this material was pressed into a transparent homogeneous pellet at 20 000 psi. For liquid samples, sodium chloride windows were used. The spectra were recorded on absorbance mode over 25 scans from which the background spectrum was automatically subtracted. The resulting data were not manipulated for a baseline correction.

To study the morphology of the particles, transmission electron micrographs (TEM) were recorded for the sample using a Philips CM200 transmission electron microscope. A

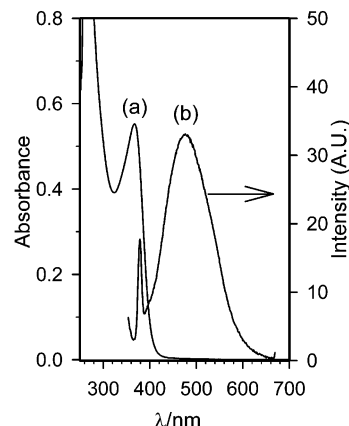


Figure 1. (a) Absorption spectrum recorded for diluted Q-CdS sol (0.5 mM) in DMSO 5 h after its preparation. (b) Emission spectrum recorded for the further diluted sol (0.1 mM). The excitation wavelength used was 340 nm.

droplet of the freshly prepared sol was dried on carbon-coated TEM grid and the measurements were carried out at 88 kV.

3.0 Results and Discussion

3.1 Formation of CdS Nanoparticles in DMSO. As described before, mixing of 10 mM $\text{Cd}(\text{OAc})_2$ and Na_2S in DMSO led to the formation of a pale yellow sol of CdS. The absorption spectrum recorded on the diluted sol (10 times) after 5 h consisted of a sharp peak at 367 ± 2 nm, as shown in Figure 1a. It is assigned to the characteristic transition for the first excitonic state of size-quantized CdS nanoparticles. Using the tight binding model,¹⁵ the average particle diameter was estimated to be 2.58 nm. A narrow full width at half-maximum (fwhm) of the peak indicated the formation of relatively monodispersed particles. The PL spectrum ($\lambda_{\text{exc}} = 340$ nm) given in Figure 1b shows two major peaks. One is the λ_{exc} dependent sharp peak at 379 nm, which showed a 3011 cm^{-1} stoke shift relative to the Rayleigh scattering. It was attributed to the Raman scattering for DMSO. The broad peak at 477 nm, more or less independent of λ_{exc} , was associated to Q-CdS. The red shift of ca. 110 nm from the absorption maxima was attributed to the recombination of excitons at the sulfur vacancies on the particle surface.^{16,17}

To confirm the formation of CdS and its crystallographic phase, an X-ray diffractogram (XRD) was recorded for the dried Q-CdS powder. A diffused broad trace as shown in Figure 2 has been reported before³ for such systems. It can be attributed to a very small grain size of the particles. Major peaks reported for hexagonal CdS¹⁸ may be associated with the two envelopes observed in XRD. The envelope at 26.5° was deconvoluted into three peaks viz. 24.8(100), 26.5(002), and 28.2(101). Using the Scherrer equation, the average particle diameter was estimated to be 4.94 nm.

A typical low-resolution TEM image obtained for the sol drop-cast onto a TEM grid is given in Figure 3. In the micrograph, the particles appear to be relatively

(15) Lippens, P. E.; Lannoo, M. *Phys. Rev. B* **1989**, *39*, 10935.

(16) Murakoshi, K.; Hosokawa, H.; Saitoh, M.; Wada, Y.; Sakata, T.; Mori, H.; Satoh, M.; Yanagida, S. *J. Chem. Soc., Faraday Trans. 1998*, *94*, 579.

(17) Brus, L. *E. J. Phys. Chem.* **1986**, *90*, 2555.

(18) Joint Committee of Powder Diffraction Standard. JCPDS File 41-1049.

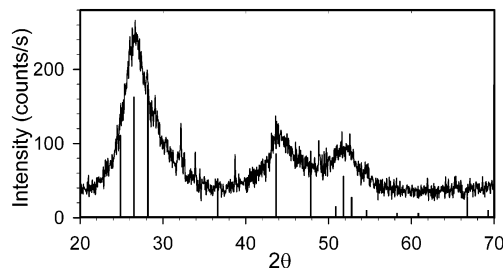


Figure 2. X-ray Diffractogram recorded on vacuum-dried Q-CdS precipitate. The vertical bars indicate the reflections reported for CdS hexagonal phase (JCPDS file 41-1049).



Figure 3. Low-resolution TEM image recorded at 88 kV for drop-casted Q-CdS sol.

monodisperse, though there is evidence of agglomeration on the TEM grid. From this micrograph, the average diameter of the particles is estimated to be 4.9 ± 0.7 nm, which matches very well with that estimated from XRD; however, it is larger than the value estimated from the tight bonding model.

3.2 Capping of Q-CdS with CD–DMSO Complex. When the sols were allowed to evolve with respect to time, the particle size was expected to increase due to a coagulation. It should have been manifested as a red shift in the UV–vis spectrum due to an increase in the band-gap associated with an increase in the particle size. The coagulation can be kinetically hindered by using surface capping agents, e.g. thiols,¹⁹ phosphines,⁹ amines,²⁰ etc. Nevertheless, the ultimate fate for a sol is inevitably sedimentation. The absorption spectra obtained for CdS sol at stipulated time intervals are given in Figure 4. The corresponding plot of the wavelength at absorption maximum (λ_{max}) vs time (inset of Figure 4) reveals that λ_{max} is blue shifted by ca. 41 nm over the course of 30 days instead of the expected red-shift for particle aggregation. This correlates to a decrease in the diameter of Q-CdS from ca. 2.58 to 1.91 nm. Moreover, there was no complementary precipitation observed at the bottom of the flask, though a decrease in the absorbance with time is apparent. The decrease in Q-CdS size with time could also be seen as the blue shift in the PL spectra. PL spectra recorded at various time intervals ($\lambda_{\text{exc}} = 340$ nm) are given in Figure 5a. It can be seen that the peak at ca. 477 nm,

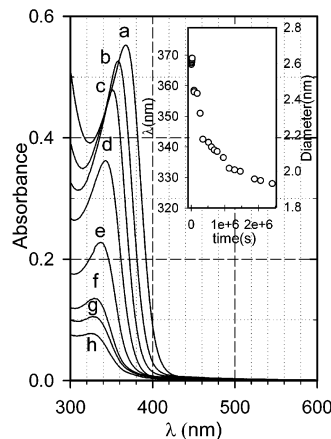


Figure 4. Evolution of the absorption spectra with time for Q-CdS sol in DMSO: (a) 5 h; (b) 1 day; (c) 4 days; (d) 5 days; (e) 9 days; (f) 22 days; (g) 30 days; and (h) 66 days after the preparation of the sol. The blue shift in spectra was attributed to a decrease in Q-CdS size due to the reaction of CdS with DMSO. Inset shows a plot of the wavelength at peak maxima (λ_{max}) vs time. The right side axis of the inset indicates the estimated particle size from the tight binding model.¹⁵

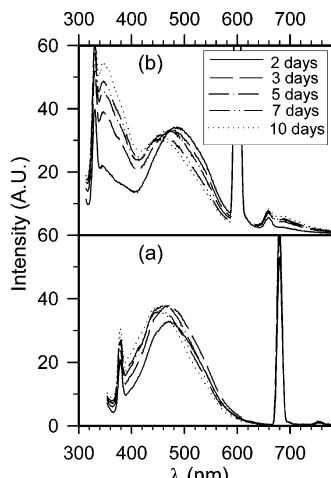


Figure 5. Evolution of the PL spectra with time for Q-CdS sol in DMSO: (a) $\lambda_{\text{exc}} = 340$ nm and (b) $\lambda_{\text{exc}} = 300$ nm. Peaks at 379 nm and 754 nm in (a) and 331 nm and 660 nm in (b) were attributed to the first- and second-order Raman scattering for DMSO. Strong peaks at 680 nm and 600 nm in case (a) and (b), respectively, were attributed to the second-order Rayleigh scattering. The broad peaks in the range of 460–480 nm are due to Q-CdS, whereas peaks at 346 nm and 686 nm were attributed to the Cd–DMSO complex.

assigned to Q-CdS, shows a blue shift with time, which is in agreement with the shift observed in the absorption spectra. Exciting the sol at 300 nm, however, revealed the presence of a new emission at 346 nm and 686 nm as depicted in Figure 5b. It can be seen that the intensities for these peaks gradually increase with time at the expense of the peak intensity ascribed to Q-CdS. These emissions could neither be attributed to CdS nor DMSO alone and thus, the formation of their complex has been envisaged, whose concentration increases at the cost of Q-CdS.

To confirm the existence of such complex on the particle surface, FTIR spectra (Figure 6b) were recorded for Q-CdS powder extracted from the sol. Additional prominent peaks at 617, 800, 1109, 1261, 1408, and 1561 cm^{-1} were noted in addition to feeble peaks which

(19) Weller, H. *Angew. Chem., Int. Ed. Engl.* **1993**, *32*, 41.

(20) Sondi, I.; Siiman, O.; Koester, S.; Matijevic, E. *Langmuir* **2000**, *16*, 3107.

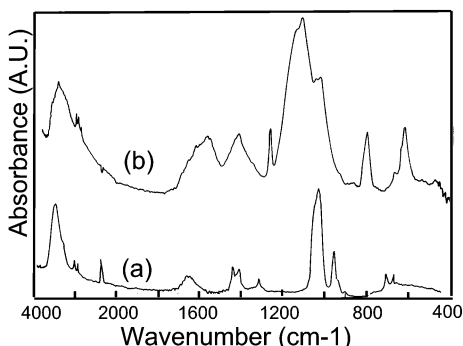


Figure 6. IR spectra recorded for (a) DMSO, and (b) KBr pellet of Q-CdS precipitate flocculated from the sol.

could be assigned to free DMSO (Figure 6a). In the range 400–4000 cm⁻¹, CdS has been reported²¹ to give very weak absorption at ca. 405 cm⁻¹, which was difficult to mark unambiguously in the current spectrum. Thus, these new prominent peaks belong to neither CdS nor DMSO, and are attributed to a form of complex between CdS and DMSO covering the native particle surface. The peaks at 1408 and 1561 cm⁻¹ could be assigned respectively to C=O, symmetric and asymmetric stretching, and attributed to the adsorbed acetate ions from cadmium acetate used in the synthesis.²² A similar observation has been previously reported by Hodes et al.¹⁴ when cadmium acetate was used as the precursor for Q-CdS synthesis. Thus, the remaining peaks at 617, 800, 1109, and 1261 cm⁻¹ can be assigned to the presence of a complex between CdS and DMSO. On the basis of IR studies reported for DMSO complexes²³ with various metal ions, including Cd²⁺ ions, the peaks at 1109 cm⁻¹ could be attributed to S=O stretching in a Cd–DMSO complex. The anti-Stoke shift of ca. 85 cm⁻¹ in S=O stretching with respect to free DMSO was attributed to the bonding of DMSO to Cd²⁺ through sulfur and not oxygen.²⁴ The observed Stoke shift in S=O stretching frequency reported by Hodes et al., however, suggested the bonding of DMSO to the surface of Cd²⁺ ions through oxygen moiety. This difference in observations could be attributed to the difference in the surface structure. Hodes et al. have reported simple chemisorption of DMSO on Q-CdS particles. However the present experiments suggest the formation of Cd–DMSO complex shell on the particle surface, which might have a bonding nature different from that of chemisorbed DMSO. The remaining peaks at 617 cm⁻¹ and 800 cm⁻¹ were assigned to symmetric and asymmetric stretching of C–S bond of the Cd–DMSO complex.²³

This leads to the obvious question of why Cd(S)–DMSO complex forms in a first place. Cd–(acetate)–DMSO complex must exist prior to addition of the sulfur

(21) Martin, T. P.; Schaber, H. *Spectrochim. Acta* **1982**, *38A*, 655.

(22) Silverstein, R. M.; Webster, F. X. *Spectrometric Identification of Organic Compounds*; 6th ed.; John Wiley and Sons: New York, 1997.

(23) Cotton, F. A.; Francis, R.; Horrocks, W. D. *J. Phys. Chem.* **1960**, *64*, 1534.

(24) Due to the electronegativity difference, the bonding molecular orbitals (MO) of the S–O moiety will have the characteristic of an oxygen atomic orbitals (AOs), whereas the antibonding MO will mainly consist of a sulfur AOs. Therefore, the complexation through sulfur will lead to an increase in the bond order, and thus, an anti-stoke shift in the stretching frequency. On the contrary, the complexation through oxygen will lead to a decrease in the bond order, and thus, will lead to a corresponding stoke shift.

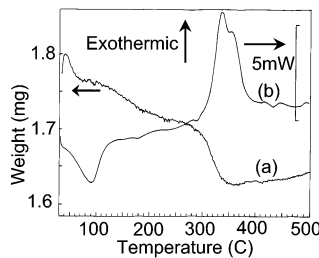
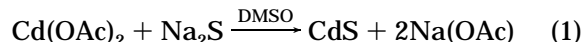
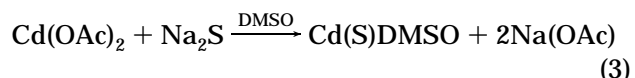


Figure 7. TGA (left axis) and DTA (right axis) thermograms recorded for Q-CdS precipitate in N₂ atmosphere. Scan rate was 10 °C/minute.

source, which should directly lead to Cd(S)–DMSO after the addition of Na₂S. Why is there formation of CdS between these two complexes? It is probable that although the formation of a Cd(S)–DMSO complex from the Cd–(acetate)DMSO complex is thermodynamically favorable, it is kinetically very slow (time scale of days). Thus, CdS is most likely the kinetically stable product (time scale of minutes), which eventually leads to Cd(S)–DMSO complex; the thermodynamically stable product. The reaction is schematically represented as follows



With a net reaction



3.3 Thermal Analysis. To understand the surface composition of Q-CdS further, the precipitate was subjected to thermal analyses in N₂ atmosphere. Figure 7 shows TG and DTA traces recorded on vacuum-dried Q-CdS powder. Three prominent weight losses were observed at endset temperatures 115 °C (2.28%), 190 °C (2.09%), and 349 °C (4.73%). The weight losses at 115 and 190 °C were accompanied by endothermic peaks in DTA at ca. 100 and 180 °C, which match the boiling points of water and DMSO, respectively. Thus, these were attributed to their physical desorption from the surface. The exothermic peak at 337 °C associated with the major weight loss at endset ca. 349 °C could be assigned to desorption/decomposition of moieties on the surface. Whereas a shoulder at 352 °C without any measurable weight change in TG could be assigned to sintering of the particles.²⁵

To resolve the exothermic processes at 337 °C, IR spectra were recorded for the Q-CdS precipitate after its isothermal heating, at stipulated temperatures, in N₂ atmosphere (Figure 8). Comparing this spectra with that of a control sample (Figure 8a), it is quite clear that the peaks assigned to C=O stretching (1408 and 1561 cm⁻¹) pertaining to the presence of acetate ions, which were prominent up to 250 °C, disappeared completely when the sample was annealed at 420 °C. However, the peaks assigned to the presence of the DMSO complex (617, 800, 1109, and 1261 cm⁻¹) remain virtually

(25) Kumar, A.; Mandale, A. B.; Sastry, M. *Langmuir* **2000**, *16*, 9299.

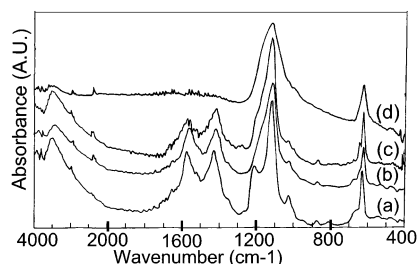


Figure 8. IR spectra recorded for Q-CdS precipitate after isothermal heating at (b) 200 °C; (c) 250 °C; and (d) 420 °C in N₂ atmosphere for ca. 2 h. (a) Control sample without any heat treatment.

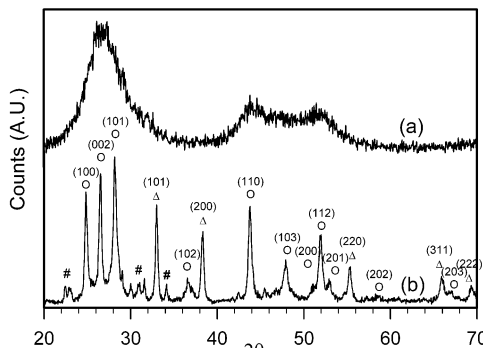


Figure 9. X-ray diffractogram recorded for Q-CdS precipitate (a) as-prepared, and (b) after annealed at 420 °C for 2 h. The peaks marked as (o) are fitted to the CdS hexagonal phase (JCPDS file 41-1049). The peaks marked as (Δ) are fitted to the CdO cubic phase (JCPDS file 5-640). Its formation was attributed to reaction of Q-CdS with acetate ions, at elevated temperature. Weak peaks marked as (#) are assigned to Cd-DMSO complex.

unchanged except for broadening due to sintering of the particles at elevated temperature. Thus, the observed weight loss at endset 349 °C is unambiguously attributed to desorption/decomposition of adsorbed acetate ions.

To further confirm this, XRD was recorded for the precipitate annealed at 420 °C (Figure 9b). Comparing the diffractogram (Figure 9a) with that obtained for the as-prepared powder (Figure 2), it is clear that two humps have been resolved into well defined peaks, which could be unambiguously assigned to hexagonal CdS.¹⁸ The prominent reflections at 2θ = 33.06°, 38.34°, 55.35°, 66.00°, and 69.35°, however, could not be assigned to CdS and could be best fitted to cadmium oxide cubic phase.²⁶ As the annealing was carried out in dry N₂ atmosphere, the air oxidation of CdS could be ruled out. Thus, the only plausible explanation is the oxidation of CdS with adsorbed acetate ions. This explanation is also in accordance with the exothermic peak at 337 °C and weight loss at endset 349 °C in DTA and TG, respectively. Weak reflections in XRD (Figure 9b, marked as '#') at 23.1°, 31.4°, and 43.1°, however, cannot be attributed to the other known phases of CdS/CdO nor to unreacted precursors/possible side products. A signature of the peaks at ca. 31.4° could also be noted in the XRD for the as-prepared sample (Figure 2 and Figure 9a). Thus, *prima facie*, these peaks could be assigned to Cd-DMSO complex.

All these observations lead to the conclusion that DMSO was not simply adsorbed on the CdS surface. It forms a CdS-DMSO complex, which was stable even at 420 °C. In addition, part of the surface was occupied by adsorbed acetate ions, as reported previously.¹⁴ These surface adsorptions are responsible for the passivation of the particle surface, and thus impart a kinetic stability to the sol.

3.4 Possibilities of the Photooxidation of Q-CdS.

Q-CdS prepared as aqueous sols have been reported to undergo photooxidation²⁷ to cadmium thiosulfate, and eventually to the sulfate, by dissolved O₂ in aqueous solutions. Therefore, the decrease in the diameter of Q-CdS as a function of time could alternatively be attributed to photooxidation of Q-CdS. The two characteristic peaks for S-O at 1109 and 617 cm⁻¹ (Figure 6b) also could be fitted to cadmium sulfate, which could be argued to form due to particle photooxidation. To understand the effect of dissolved O₂, sols were also prepared in N₂ and O₂ atmospheres. XRD and FTIR spectra recorded (Supporting Information, Figures 2S and 3S) for these samples were found to resemble those recorded for samples in air. Even in oxygenated sol, we did not observe reflections in XRD which could be fitted to any of the phases of cadmium sulfate, thiosulfate, or CdO. The remaining filtrate after the extraction of sols did not lead to a characteristic BaSO₄ precipitate when treated with BaCl₂. Thus, the presence of dissolved sulfates in the solution has also been ruled out. The weight loss and change in enthalpies in thermal analysis also did not support the presence of sulfate or thiosulfate. All these experimental facts rule out the possibility that the decrease noted in Q-CdS diameter was due to the photooxidation. Water, which is reported to play the major role in the reaction mechanism of photooxidation,²⁷ was absent in the present investigation. This could be a possible reason for the absence of photooxidation in the sols prepared in DMSO.

3.5 Kinetics of Reaction Between Q-CdS and DMSO.

As described above, the reaction between Q-CdS and DMSO was manifested as a decrease in the absorbance for Q-CdS. The systematic changes in the absorption spectra were used to estimate the rate constant and order of the reaction between CdS and DMSO.

Equation 2 could be written as



where *a* and *b* are arbitrarily chosen coefficients as the exact reaction stoichiometry is unknown, and *k* is the corresponding rate constant. The particles are extremely small (a few nm in diameter). Thus, as a first approximation they can be treated as giant molecules. Moreover, the sol is homogeneous, and therefore, an isotropic collisional cross section can be assumed. Thus, using the approximation of homogeneous kinetics, the rate law can be written as

$$-\frac{1}{a} \frac{d[\text{CdS}]}{dt} = k[\text{CdS}]^n \cdot [\text{DMSO}]^m \quad (5)$$

where *n* and *m* are orders of the reaction with respect

(26) Joint Committee on Powder Diffraction Standard. JCPDS File 5-640.

(27) Awatani, T.; McQuillan, J. *J. Phys. Chem. B* **1998**, *102*, 4110.

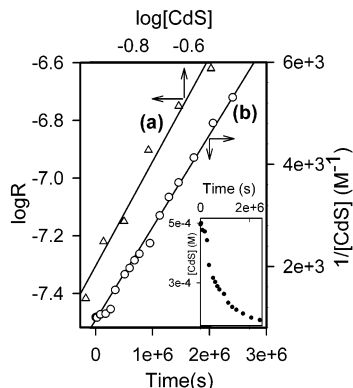


Figure 10. Plots for second-order fittings for the reaction kinetics between CdS and DMSO: (a) log–log plot for rate of reaction vs [CdS]; (b) plot of $1/[CdS]$ vs time. Inset shows exponential decay of [CdS] with time. The concentration of CdS was determined from the absorbance, using reported value of the molar absorptivity for CdS.

to $[CdS]$ and $[DMSO]$, respectively. Being the solvent, DMSO is in far excess and its concentration remains virtually unperturbed in the experimental time frame. Thus, eq 5 can be simplified to

$$R = -\frac{d[CdS]}{dt} = K[CdS]^n \quad (6)$$

where $K = a[DMSO]^m$ and R are the apparent rate constant and rate of the reaction, respectively.

If the reaction obeys eq 6, then, as per the van't Hoff graphical method,²⁸ a plot of $\ln(R)$ vs $\ln[CdS]$ at a stipulated time interval should yield a straight line with a slope and intercept equal to n and K , respectively. A plot of the concentration of CdS vs time is depicted in the inset of Figure 10, which shows an exponential decay. The corresponding log–log plot for (R) vs $[CdS]$, shown in Figure 10a, gives a straight line ($r^2 = 0.97$) with a slope and intercept equal to 1.76 and -5.65 , respectively. From this, the reaction can be assumed to be second order with respect to $[CdS]$. From the intercept, K was estimated to be $2.23 \times 10^{-6} \text{ L mol}^{-1} \text{ s}^{-1}$. A

(28) Steinfield, J. I.; Francisco, J. S.; Hase, W. L. *Chemical Kinetics and Dynamics*; Prentice Hall: New York, 1989.

plot of $1/[Q\text{-CdS}]$ vs time also fitted well ($r^2 = 0.99$) to a straight line (Figure 10b), which is in accordance with a second-order rate law with respect to $[CdS]$. From the slope, K was estimated to be $1.81 \times 10^{-6} \text{ L mol}^{-1} \text{ s}^{-1}$ which is in good agreement with that determined by the van't Hoff graphical method. Being a second-order decay, these results could have been attributed to the coagulation of electro-neutral species on the basis of Smoluchowski coagulation mechanism.²⁹ However, no evidence of precipitation was observed even after allowing the sol to evolve for months. Therefore, this possibility can be ruled out.

4.0 Conclusions

This report is, to the best of our knowledge, the first observation of a reaction between Q-CdS and DMSO. On the basis of data obtained using UV-vis, FTIR spectroscopy, thermal analysis, and XRD, the formation of a stable CdS–DMSO complex as a shell on Q-CdS surface has been proposed. Acetate ions were also found to adsorb on the particle surface. The reaction between Q-CdS and DMSO was fitted to the second-order kinetic mechanism with an apparent rate constant equal to ca. $2 \times 10^{-6} \text{ L mol}^{-1} \text{ s}^{-1}$. These results suggest that alkyl sulfoxides, e.g., DMSO, can be used to stabilize the particles in a manner similar to alkyl phosphine oxides. In future studies, the use of long chain alkyl sulfoxide instead of methyl sulfoxide is proposed.

Acknowledgment. We thank Nilesh Kulkarni (TIFR), Prashant Dikshit (Medlar Laboratory), and Prof. Samazdar (RSIC), for XRD, thermal analyses, and TEM, respectively. We also thank Bernadette Quinn (Helsinki University of Technology, Finland) and Nanda Haram (TIFR) for the useful discussion. The financial support for this research by the Department of Atomic Energy, India (DAE Young Scientist Research Award, Project 20-1-98 R&D 824) is gratefully acknowledged.

Supporting Information Available: Diagram of experimental setup, and FTIR spectra and XRD for precipitates of sols prepared in N_2 and O_2 atmospheres. This material is available free of charge via the Internet at <http://pubs.acs.org>.

CM020761W

(29) Nielsen, A. E. *Kinetics of Precipitation*; Pergamon Press: Oxford, U.K., 1964.